

Determination of sulfur in fossil fuels by isotope dilution electrothermal vaporization inductively coupled plasma mass spectrometry

Lee L. Yu,* William Robert Kelly, John D. Fassett and Robert D. Vocke

Analytical Chemistry Division, National Institute of Standards and Technology, Gaithersburg, MD 20899–8391, USA

Received 16th November 2000, Accepted 21st December 2000
First published as an Advance Article on the web 26th January 2001

www.rsc.org/jaas

The determination of S by solution nebulization quadrupole inductively coupled plasma mass spectrometry (ICP-MS) is difficult because of interferences from oxygen dimer ions. The large $^{16}\text{O}_2^+$ ion current from the solvent water is a serious interference at ^{32}S , the most abundant of the four isotopes, and precludes its measurement. The isotopic composition of S varies in nature as a consequence of natural mass fractionation; therefore, high accuracy isotope dilution mass spectrometric (IDMS) determination of sulfur requires that the ratio of $^{32}\text{S}/^{34}\text{S}$ be measured, for the two isotopes represent over 99% of natural sulfur. In this work, electrothermal vaporization was used to generate a water-free aerosol of the sample. Non-solvent sources of oxygen were investigated and the spectral background minimized. Further reduction of the oxygen dimer was achieved by using nitrogen as an oxygen-scavenger in the argon plasma. The isotope ratio of $^{32}\text{S}/^{34}\text{S}$ was used for the determination of S by IDMS. The repeatability of the $^{32}\text{S}/^{34}\text{S}$ ratio in terms of the relative standard error (95% confidence level) of 6 replicate measurements of the spiked and the unspiked samples was about 0.3% and 0.7%, respectively. The detection limit of the method was 4 ng g^{-1} . Sulfur in two fossil fuel reference materials was measured and the results were in good agreement (within 0.3%) with those obtained by the more precise thermal ionization mass spectrometry (TIMS) method.

Sulfur is an important contaminant in the environment. Combustion of fossil fuels is the primary source of anthropogenic S compounds released into the atmosphere, and the Environmental Protection Agency (EPA) has progressively lowered the permissible levels of S in fossil fuels. A case in point is the recent EPA proposal to lower the legal limits of S in gasoline from the current $330\text{ }\mu\text{g g}^{-1}$ to about $30\text{ }\mu\text{g g}^{-1}$ by 2004.¹

Sulfur is also an important element in metallurgy. The physical and chemical properties of steels and alloys are significantly affected by small changes in S concentration. In most metals and alloys, intergranular brittleness is associated with strong segregation of harmful impurities like S and P to grain boundaries, causing or exacerbating brittleness of the material.² Many efforts are made to reduce S in alloys and steels to eliminate these effects. It was estimated that, with the advancement of refining techniques, the refining limit of steel would be below $0.6\text{ }\mu\text{g g}^{-1}$ for S by the year 2000.³ These developments in the industry challenge analytical capabilities for sensitive and accurate sulfur measurement.

At low concentrations, S is an extremely difficult element to quantify accurately. An accurate technique measures the true number of analyte atoms in the sample. This requires that the sources of random and systematic error be evaluated, the proper corrections be made to the measured data and all sources of uncertainty be assessed and clearly stated.⁴ Isotope dilution (ID) is considered an accurate technique and isotope dilution determination of S by thermal ionization mass spectrometry (TIMS) has been used alone to certify S in a variety of Standard Reference Materials (SRM[®]) with concentrations from 0.4 to $10^4\text{ }\mu\text{g g}^{-1}$.^{5,6} The instrument detection limit of TIMS is estimated to be around 1 pg of S, but the procedural blank of about $0.25\text{ }\mu\text{g}$, resulting from the chemical pretreatment of the sample, is the current limitation.⁶

Inductively coupled plasma mass spectrometry (ICP-MS) has, essentially, 100% ionization efficiency for most metal

elements and can detect and quantify almost all elements. Elements with two or more stable isotopes may be quantified by using isotope dilution, which uses an artificially enriched isotope as an internal standard. One of the limitations of ICP-MS is caused by the non-selective ionization process. Atomic or molecular ions interfere for some elemental nuclides. Sulfur, whose ionization efficiency is about 14% in the plasma, is one of several elements that are particularly prone to isobaric interferences and are therefore difficult to measure. It has four isotopes at nominal masses 32, 33, 34 and 36, with nominal abundances of 95%, 0.75%, 4.2% and 0.02%, respectively. Oxygen-containing ions and argon ions interfere with each isotope of S: $^{16}\text{O}_2^+$, $^{16}\text{O}_2^1\text{H}^+$, $^{16}\text{O}^{18}\text{O}^+$, and $^{36}\text{Ar}^+$ at masses 32, 33, 34 and 36, respectively. These interferences preclude the measurement of sulfur at these masses by aqueous solution nebulization ICP-MS. Measuring the intensities of SO^+ species instead of S^+ has been reported to circumvent the interferences at S masses.^{8,9} However, an ion exchange separation was required to minimize the interferences from $^{48}\text{Ca}^+$, $^{50}\text{Cr}^+$, $^{50}\text{Ti}^+$, $^{50}\text{V}^+$, $^{36}\text{Ar}^{12}\text{C}^+$, $^{31}\text{P}^{17}\text{O}^+$, $^{31}\text{P}^{16}\text{O}^1\text{H}^+$ and $^{38}\text{Ar}^{12}\text{C}^+$,⁹ and the sensitivity at a SO^+ mass was about 1/50 of that at the corresponding S^+ mass.⁸ As a result, a detection limit of $0.6\text{ }\mu\text{g mL}^{-1}$ was obtained at mass 48,⁸ relative to the $0.07\text{ }\mu\text{g mL}^{-1}$ obtainable at mass 34.¹⁰ Commercial ICP source high-resolution sector-field mass spectrometers (HR-ICP-MS) have resolutions ($m/\Delta m$) greater than 3000 and readily resolve interferences at ^{32}S , ^{33}S and ^{34}S . Still, HR-ICP-MS is unable to resolve the overlap of $^{36}\text{Ar}^+$ with $^{36}\text{S}^+$. Sector field HR-ICP-MS has been used for the determination of S by external calibration,¹¹ as well as by isotope dilution analysis.¹² A detection limit of 0.01 ng g^{-1} and a $^{34}\text{S}/^{32}\text{S}$ relative precision of 0.04% was achieved by using ID-HR-ICP-MS.¹² Nevertheless, sector field HR-ICP-MS is costly and thus fewer instruments are available relative to quadrupole ICP-MS. More recently, Mason *et al.* reported the measurement of S in water samples by using a hexapole

collision cell ICP-MS instrument.¹³ The isobaric interference at mass 32 was reduced to $<10^5$ counts s^{-1} by using a mixture of He–Xe–H₂ in the hexapole region, and the sulfur detection limit was about 20–50 ng mL⁻¹.¹³ While the use of H₂ dramatically reduced the isobaric interference at mass 32, the gas mixture could not be used for the measurement of ³⁴S/³²S because H₂ deteriorated the accuracy of the measurement.¹³

The oxygen in the interfering polyatomic ion species at masses 32, 33 and 34 is primarily from the water solvent, and the intensities of these ions may be minimized by introducing the sample as a water-free aerosol.¹⁴ Electrothermal vaporization (ETV) is an alternative sample introduction technique, in which the sample is desolvated prior to being introduced into the plasma. The desolvation of the sample and the ionization of the analyte can be optimized independently such that the water loading of the plasma is minimized. The vaporization mechanism of S in ETV was studied by Gregoire and Naka, who were able to reduce the spectral background at masses 32, 33 and 34 to about 50 000, 1 500 and 1 000 counts s^{-1} respectively.¹⁵ The complete removal of solvent water from the sample matrix was not possible; consequently, a background as high as 200 000 counts s^{-1} for samples was observed at mass 32, rendering this mass useless for S analysis.¹⁵ Naka and Gregoire successfully demonstrated that the ID-ICP-MS determination of $\mu\text{g g}^{-1}$ levels of S in steel was possible by using the ratio of ³³S/³⁴S with ³⁴S as a tracer.¹⁶ However, sulfur is one of the few elements whose isotopic composition varies in nature. An accurate determination of S by isotope dilution mass spectrometry (IDMS) requires that the isotopic composition of S in the sample be determined. IDMS results based on the ratio of ³³S/³⁴S alone may have large biases if the exact composition of the S is unknown.¹⁷ The ³²S/³⁴S isotope ratio should be used in the quantification of S by IDMS to minimize the impact of the variable sulfur compositions on the overall measurement uncertainty.¹⁷

The elimination of oxygen in the plasma is extremely difficult using the ETV sampling system, because residual gaseous water and oxides of the sample matrix will be carried into the plasma during the vaporization of the analyte.¹⁵ However, the relative concentration of the polyatomic ions of oxygen may be manipulated advantageously to optimize the signal-to-noise (S/N) and signal-to-background (S/B) ratios at S masses of interest by altering the composition of the plasma support gas.¹⁸ This was demonstrated by Lam and Horlick, who used N₂ as a scavenger for oxygen to alleviate the isobaric interference of ⁴⁰Ar¹⁶O⁺ on ⁵⁶Fe⁺ by adding a small amount of N₂ to the Ar plasma gas.¹⁹ Logically, similar beneficial effects should result from the use of the mixed gas plasma for the determination of S. However, the use of the mixed gas plasma for S analysis has never been reported in the literature, probably because the plasma water loading of a solution nebulization ICP-MS is too high for N₂ to be effective in reducing the background at S masses.

The effectiveness of the Ar–N₂ plasma in minimizing the O₂⁺ species at reduced plasma water loading (*i.e.*, by using the ETV sampling system) is the subject of research reported here. This paper discusses the impact of N₂ as an oxygen scavenger in the measurement of S by using ETV-ICP-MS, with an objective of using ³⁴S/³²S for the quantification of S by IDMS.

Experimental

Reagents and equipment†

A PE Sciex Elan 5000 ICP-MS (Thornhill, Ontario, Canada) and a Perkin Elmer HGA-600MS electrothermal vaporization system equipped with an AS-60 autosampler (Norwalk, CT,

USA) were used for this work. Pyrolytic graphite coated tubes were used throughout. An N₂–Ar plasma was produced by adding N₂ to the outer flow of the plasma. The flow of N₂ was controlled with a Model 603 tapered rotameter flow meter from Matheson Gas Products (Secaucus, NJ, USA). A Convectron Model 275 vacuum gauge from Granville-Phillips (Boulder, CO, USA) was installed to monitor the pressure in the interface region. Injection ports for introducing several microliters of gas were installed in the plasma and the injector flows. Each port was made of a 10 mm od by 3 mm rubber septum set in the middle opening of a 9.5 mm od Swagelok tee. Ten μL and 50 μL micro-syringes from Hamilton Co. (Reno, NV, USA) were used for gas sample introduction. Table 1 identifies the instrument parameters used for isotope ratio measurements.

The enriched ³⁴S tracer was obtained from Mound Laboratory (Miamisburg, OH, USA). The 100 $\mu\text{g g}^{-1}$ KOH matrix modifier solution¹⁵ was prepared with AR grade pellets that contained $<0.0005\%$ SO₄ from Mallinckrodt (Paris, Kentucky, USA). All calibration standards were prepared by appropriate dilutions of SRM 3154 Sulfur Spectrometric Solution from the National Institute of Standards and Technology (NIST, Gaithersburg, MD, USA) in 0.2 mol L⁻¹ HNO₃ prepared at NIST by sub-boiling distillation. Sample solutions of SRM 2719 Petroleum Coke and SRM 2724b Diesel Fuel contained a similar acid concentration.

Procedure

The S/N and S/B ratios as a function of nitrogen concentration in the plasma were studied by measuring the signal intensity of a blank and a 0.25 $\mu\text{g g}^{-1}$ S solution in a plasma that contained volume fractions of about 0%, 1.3%, 2.5%, 3.8%, 5.0% and 6.3% N₂. Nitrogen was introduced to the plasma through the plasma flow of the Ar gas. The sample was introduced into the ICP-MS with ETV; the parameters for the ETV are listed in Table 1. The noise as the peak-to-peak intensity and the background as the average intensity are calculated from a 5 s measurement period of a blank.

Sources of oxygen that resulted in the spectral background were studied by connecting the nebulizer Ar flow directly to the injector at the base of the torch. The normal sample introduction systems were not used. In this mode of operation, the oxygen in the plasma is from the plasma gas alone (dry plasma). Carbon dioxide was used as a tracer to study the entrained air in the plasma as a source of oxygen. A stream of

Table 1 Instrument parameters

<i>Inductively coupled plasma mass spectrometer:</i>	
Spectral resolution	0.8 amu (normal)
Rf Power	1000 W
Plasma flow rate	15.9 L min ⁻¹
Auxiliary flow rate	0.900 L min ⁻¹
Carrier flow rate	1.400 L min ⁻¹
<i>Electrothermal vaporizer:</i>	
Sample volume	20 μL
Modifier (100 $\mu\text{g g}^{-1}$ KOH) volume	10 μL
Internal Ar flow rate	300 mL min ⁻¹ before vaporization step
<i>ETV temperature:</i>	
Dry (ramp, hold)	100 °C (10 s, 30 s) 200 °C (30 s, 30 s)
Pyrolysis (ramp, hold)	400 °C (30 s, 30 s)
Vaporization (ramp, hold)	1600 °C (0 s, 6 s)
Purge (ramp, hold)	2600 °C (1 s, 5 s)
<i>Data acquisition:</i>	
Dwell time	20 ms
Sulfur isotopes monitored	32, 34
Scan mode	Peak hop transient
Points per spectral peak	1
Signal measurement	Integrated signal pulse

†Certain commercial instruments are identified in this paper to specify adequately the experimental procedure. Such identification does not imply recommendation or endorsement by the National Institute of Standards and Technology, nor does it imply that the equipment identified is necessarily the best for the purpose.

CO₂ was directed at the sampler cone orifice at about a 70° angle to the axial channel of the plasma. The 3 mm id nozzle of the CO₂ flow was about 5 cm from the sampler orifice. The flow rate of CO₂ was gradually increased from 0 to about 20 L min⁻¹ while the intensity at mass 44 was measured. The presence and the absence of a leak at the thread mount of the sampler cone was investigated by using the Type I Ni cone (PN N812-2001, Perkin-Elmer) with rubber gasket and Type II Ni cone (PN WE01-3087, Perkin-Elmer) with Al gasket alternately while observing the oxygen background at mass 32. Apiezon vacuum grease was occasionally used on the thread of the sampler cone.

The capacity of the 5% N₂-95% Ar plasma to minimize the interferences of the matrix-source oxygen was studied by using gaseous oxygen to simulate the effect of oxygen from the matrix. The sensitivity of oxygen and the detection limit of S at mass 32 were determined. To measure the sensitivity of oxygen, a calibration curve of oxygen was constructed by injecting gaseous oxygen through a septum installed in the nebulizer flow into the plasma in volumes of 0, 10, 20, 30, 40 and 50 μL. Three replicate measurements were made at each oxygen level.

Calibration curves of S were constructed with solutions containing 0, 0.097, 0.18, 0.25, 0.34, 0.44 and 0.53 μg g⁻¹ S. The detection limit was calculated as the concentration giving a signal equivalent to 3 times the noise, and the standard deviation of 11 repetitive measurements of the background intensity was obtained. All statistical intervals are given at a 95% confidence interval unless otherwise specified.

The samples of SRM 2719 Petroleum Coke and SRM 2724b Diesel Fuel were digested in Carius tubes using procedures described elsewhere.⁶ One gram of the total 6 g digest from each sample was taken for ETV-ICP-MS measurements. The remaining digest was reduced and precipitated as As₂S₃ for the determination of S by TIMS.⁶

For the IDMS determination of S by using the ETV sampling system, the plasma of the ICP-MS instrument was lit with the N₂ flow set at 0. The N₂ flow was increased to 0.8 L min⁻¹ and the instrument was allowed to warm up for about 2 hours before any measurements were made. Each digest from the Carius tube was diluted semiquantitatively with deionized water to give intensities between 10⁵ and 10⁶ counts s⁻¹ at mass 32. The corresponding mass fraction of ³²S in the dilute solution was about 0.25 to 0.5 μg g⁻¹. An S standard enriched with ³⁴S was used to correct for the mass bias of the ICP-MS instrument. The ³²S/³⁴S ratio of the mass bias standard was accurately determined by TIMS to be 1.5764. The mass bias standard was measured after every 4 samples. Six replicate measurements were made for each sample.

Results and discussion

Isotope selection

Each of the 4 sulfur isotopes, at nominal masses of 32, 33, 34 and 36, suffers isobaric interferences from the background species of the plasma. Sulfur 36 is irresolvable from the elemental isobar of ³⁶Ar⁺, a predominant species in the plasma even at 0.34% relative isotopic abundance; therefore, the ³⁶S cannot be used in the IDMS measurement of S. As a result, the sulfur concentration in the sample is estimated by using the isotope ratios of the remaining three isotopes at masses 32, 33 and 34.¹⁷ In practice, the sulfur concentration can be estimated from the ratio of just two isotopes. The uncertainty of the estimate depends on the isotopes of the ratio measurement, and it is at a minimum when sulfur is estimated from the ratio of ³²S/³⁴S,¹⁷ the two most abundant isotopes representing greater than 99% of natural sulfur.

In recent theoretical work, the merit of measuring the two independent ratios from the three isotopes of ³²S, ³³S and ³⁴S is compared to that of measuring just ³²S/³⁴S.¹⁷ The relative

uncertainty of the concentration estimate from the ratio of ³²S/³⁴S is <0.04%, and that from using both ratios ³²S/³³S and ³²S/³⁴S is <0.005%.¹⁷ In contrast, the uncertainty of the isotope ratio measurement using the ETV sampling system is about 0.5%, as shown later. It is obvious that the uncertainty of the final result is determined by the overriding 0.5% uncertainty of the measurement. The lack of measurement of ³³S insignificantly contributes to the overall uncertainty of the result. Moreover, the uncertainty of an isotope ratio measurement using the ETV sampling system increases as the number of isotopes measured increases. This is a natural consequence of the limited sampling possible of the time-intensity profile produced during the ETV process. Therefore, ³²S and ³⁴S were selected for quantification in this work, and the intensity at mass 33 was occasionally measured for diagnostic purposes only.

N₂ in the plasma

The addition of nitrogen into an Ar plasma alters its chemical and physical properties,¹⁸ and hence the performance of the plasma in terms of the sensitivity, S/B and S/N.²⁰ The S signal, O₂ background and the background noise as a function of the N₂ concentration in the plasma are shown in Fig. 1. The intensity of S and the background decreased sharply with the increase of N₂ in the plasma until the concentration of N₂ reached about 2%. Then the sulfur intensity increased gradually while the background intensity experienced a much slower rise. As the concentration of N₂ in the plasma gas was increased, the brightness of the plasma increased and its size decreased, which corroborated observations of others.^{19,20} The decrease in the axial dimension was more pronounced than that in the radial dimension until N₂ reached a volume fraction of about 2% in the plasma flow. Then the axial dimension of the plasma appeared stabilized while the radial dimension of the plasma experienced rapid shrinkage. The decrease of the S intensity at N₂ < 2% is consistent with the description by Craig and Beauchemin,²⁰ and it is probably a result of the initial radiation zone (IRZ)²¹ moving away from the sampler orifice.²⁰ The rise in intensities at N₂ > 2% corresponded to a more rapid shrinkage of the plasma in the radial rather than axial dimension. A tentative explanation is that the decrease of the diameter of the toroidal plasma exerted a pinch effect on the center channel of the plasma, resulting in an increased temperature and hence enhanced ionization efficiency of the analytes in the center channel.

Two factors were probably responsible for a more rapid rise of the intensity of S over that of the background as the N₂ increased to >2%. First and foremost, the increase of N₂ in the plasma increased the amount of oxygen being scavenged, resulting in a decreased concentration of O₂⁺. Second, the ionization potential (IP) of S (10 eV) is lower than O₂ (12 eV) and, therefore, an increase in temperature may give rise to a larger intensity increase in the former than the latter. Consequently, the S/B (Fig. 2) and S/N (Fig. 3) exhibit a monotonic increase with the increase of the N₂ in the plasma. This is consistent with the observations by Craig and Beauchemin,²⁰ who noted that in a N₂-Ar plasma the S/N

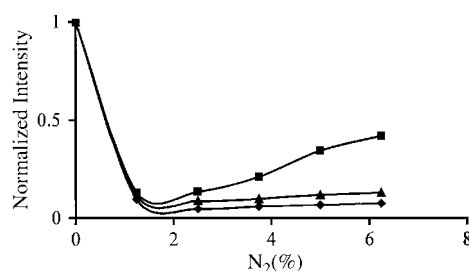


Fig. 1 Effect of N₂ flow on S signal and background at mass 32: (■) sulfur signal, (▲) background, and (◆) noise.

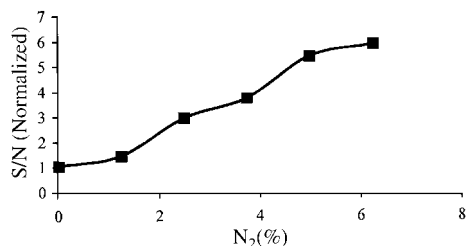


Fig. 2 Effect of N₂ flow on S/N at mass 32.

increased at the masses that were affected by spectral interferences. It appears that the S/N improves continuously with increasing N₂ concentration. Unfortunately, at N₂ volume fractions higher than 6.25% the plasma became unstable. For instance, a slight disturbance in the plasma gas resulting from the activation of the pneumatic valve of the ETV would douse the plasma. Furthermore, due to the higher thermal conductivity of N₂¹⁸ relative to Ar, the interface and the torch box of the instrument heated up rapidly at N₂ > 5%, which triggered frequent instrument shut down. Therefore the N₂ concentration was optimized at 5% for this work.

Minimizing the background

The plasma background at mass 32, presumably resulting from ¹⁶O₂⁺, was of the order of 10⁴ counts s⁻¹ for a dry Ar plasma without the ETV attachment. This background adversely impacts on the measurement at mass 32 in two ways: first it results in an additive interference to the signal and reduces the linear dynamic range at the affected mass, although the interference can generally be subtracted numerically by using the reading of a blank. Second, the fluctuation of the background, which normally is proportional to the magnitude of the background, contributes to the noise of the measured signal. Therefore, the background must be minimized for accurate and precise measurements of S at mass 32. To minimize the background at the sulfur mass, the sources of the oxygen must be located. In the absence of solvent water, the possible sources of oxygen are air entrained by the plasma gas, air leaking at the sampler cone and oxygen in the plasma gas. Each of the aforementioned sources of oxygen was examined and is discussed below.

The presence or absence of entrained air by the plasma was determined by using carbon dioxide as a tracer. The carbon dioxide ion is readily detected at mass 44 by ICP-MS since the ionization potential of CO₂ (13.8 eV) is about the same as that of O (13.6 eV) whose ion peak is a prominent feature in ICP-MS spectra. Fig. 4 shows the response at mass 44 as a function of an increased flow of CO₂ directed at the plasma. If a significant amount of the ambient air was entrained by the plasma, a corresponding increase of the intensity at mass 44 would be expected. The fact that the intensities at mass 44 did not correlate with the increasing CO₂ flow rates from 0 to about 15 L min⁻¹ (Fig. 4) suggests that the entrained air by the plasma was negligible. At CO₂ flow rates of >15 L min⁻¹, the linear velocity of the gas was greater than 30 m s⁻¹. In contrast, the normal flow around the plasma resulting from the exhaust was

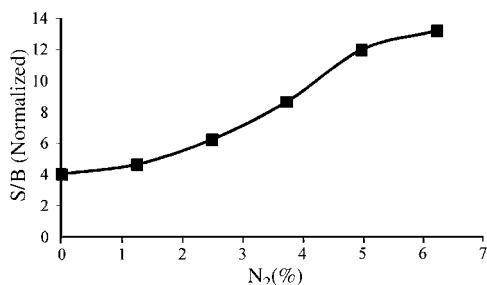


Fig. 3 Effect of N₂ flow on S/B at mass 32.

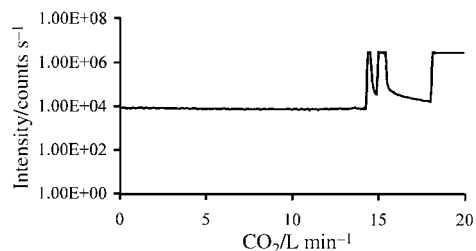


Fig. 4 Intensity of CO₂⁺ as a function of CO₂ flow: at <14 L min⁻¹, CO₂ had no effect on the plasma; from 14 to 17 L min⁻¹, CO₂ disrupted the plasma flow intermittently; at >17 L min⁻¹, CO₂ disrupted the plasma flow constantly.

only about 0.06 m s⁻¹. The plasma plume flickered at these flow rates of CO₂. The sudden increase of the intensity at mass 44 was probably a result of the stream of CO₂ disrupting the plasma flow that shielded the injector flow from the ambient air.

The second possible source of oxygen is a leak around the thread mount of the sampler cone, as was discovered in the course of these investigations. The typical baseline intensity at mass 32 was about 30 000 counts s⁻¹ when a Type I Ni sampler cone with a rubber gasket was used. The rubber gasket deteriorates after about 40 h of normal use with a 1 kW argon plasma, because of the heat from the plasma conducted by the sampler. The degradation of the rubber gasket accelerated when a 1 kW, 5% N₂-Ar plasma was employed, because the temperature at the sampler cone was even higher. The rubber gasket cracked to pieces after about 8 h of use. A slight decrease of the baseline to about 20 000 counts s⁻¹ was realized when a Type II Ni sampler cone and a new Al gasket were used. A slackening developed in the fitting of the sampler following its first use. After the sampler cone was tightened again the background intensity was further decreased to about 6000 counts s⁻¹. No further reduction of the background intensity was noticeable when Apiezon vacuum grease was applied at the thread mount of the sampler cone, suggesting that the leak was remedied. To observe the impact of the leak on the background at mass 32, the sampler cone was loosened from the optimum by turning it about 5° left. The baseline intensity at mass 32 increased from about 6000 to over 10⁵ counts s⁻¹.

It is of interest to speculate how the leak around the sampler cone translated into an elevated background at mass 32. The interface pressure was little changed at about 0.31–0.32 kPa throughout the experiment with different types of sampler cones. At these pressures the Mach disk was about 11–12 mm behind the 1 mm diameter orifice of the sampler cone.²² The sampler-skimmer separation was about 6.1 mm; therefore, the skimmer orifice was well within the Mach disk. If the supersonic shock structure is impervious to the background gas, the background intensity would not have been affected by this small leak. Campagne²³ suggested that the shock structure of the supersonic jet was porous. Consequently the optimum sampler-skimmer separation was found at 2/3 the distance of the Mach disk²² where the diffusion of the background gas into the ion beam was minimized. A leak around the sampler would increase the oxygen concentration in the background gas. The increase of the intensity at mass 32 caused by the small leak around the sampler cone must result from the background gas in the interface penetrating the supersonic shock structure and interacting with the ion beam.

The background intensity was reduced when the Type II Ni cone and Al gasket were used and is probably attributable to the thermal properties of these materials. The thermal expansion coefficients (TEC) for Al and Ni are 24 × 10⁻⁶ K⁻¹ and 13 × 10⁻⁶ K⁻¹, respectively. Since Al expands faster than Ni when heated, a tighter seal results as the temperature of the sampler assembly increases. The expansion of the Al gasket under the heat of the plasma

coincidentally molds the soft Al gasket to mesh with the surfaces of the sampler and the interface. The gaps resulting from the slight mismatch between the surfaces of the sampler, the interface and the Al gasket at the ambient temperature is thus minimized at the operating temperature of the plasma. A small gap develops after the plasma is turned off and the sampler cools. The subsequent tightening adjustment of the sampler compensates for the gap and results in a better vacuum seal. Therefore, the Type II Ni cone with Al gasket was used for all other experiments.

The remaining background of about 6000 counts s^{-1} is probably from the impurities in the plasma gas. The specification of the liquid Ar used lists O_2 and H_2O impurities at less than $4 \mu L L^{-1}$ and $3.5 \mu L L^{-1}$, respectively. Higher purity Ar would be expected to reduce the background further, but this approach was not pursued because high purity Ar is primarily supplied as cylinder gas, and the limited capacity and higher cost of the high-purity cylinder gas makes it an impractical alternative to liquid Ar.

Nitrogen is known to be a scavenger for oxygen that minimizes the interferences at masses affected by oxides. However, the effect of nitrogen on the background at mass 32 is two-fold. On the one hand, the N_2 scavenges O_2 in the plasma to form NO^+ , which increases monotonically with the concentration of N_2 in the plasma (Fig. 5). Therefore, the N_2 -Ar mixed gas plasma minimizes the O_2^+ in the plasma and thus the background at mass 32. On the other hand, the oxidation product formed by nitrogen and a minor isotope of oxygen, $^{14}N^{18}O^+$, also increases with the concentration of N_2 in the plasma and this interferes with $^{32}S^+$. Fortunately, $^{14}N^{18}O^+$ accounts for $<0.2\%$ of all NO^+ species. As a result, the decrease of $^{16}O_2^+$ more than offsets the increase of $^{14}N^{18}O^+$, and the overall effect of adding N_2 to the plasma is a significant decrease of the background at mass 32. For this experiment, the background at mass 32 decreased from about 6000 to about 1600 counts s^{-1} when N_2 in the plasma gas was increased from 0 to 5%. The contribution of NO^+ to the background at mass 32 can be estimated by using the curve in Fig. 5. The NO^+ intensity at mass 30 is about 200 000 counts s^{-1} in a 5% N_2 -Ar plasma. As a result, only 400 counts s^{-1} of the 1600 counts s^{-1} background at mass 32 is attributable to $^{14}N^{18}O^+$.

Oxygen from the sample

Molecular oxide species that form during vaporization are a significant source of oxygen. Unlike the sources of oxygen discussed earlier, this source of oxygen results in a positive bias at the affected mass that cannot be corrected for by subtracting the reading of the blank. Although the ETV sampling system facilitates the removal of oxides in the sample matrix by allowing independent optimization of drying and pyrolysis, a small amount of oxygen in the forms of water, metal oxide, carbon monoxide, or salts of oxy-acids is unavoidably introduced into the plasma with the analyte.^{15,24,25}

The 5% N_2 -Ar plasma proves effective in minimizing the

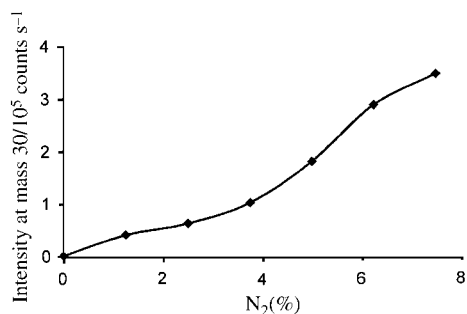


Fig. 5 Intensity of NO^+ as a function of N_2 % in the plasma.

oxygen background at mass 32; however, the scavenging effect of N_2 is limited by the concentration of N_2 in the plasma and the kinetic and dynamic parameters that affect the nitrogen-oxygen interaction. It is conceivable that, with the increase of the oxides in the sample matrix, the oxygen in the plasma will eventually exceed the limit of the scavenging capacity of a plasma with a given N_2 concentration. Keeping the total oxygen in the plasma below this limit is critical for an accurate determination of S. Therefore, the limit of oxygen in the plasma above which the contribution of O_2^+ at mass 32 becomes detectable was investigated.

An estimate of this oxygen limit in the plasma was made by comparing the sensitivity factor of oxygen to the detection limit of S in terms of intensity in the 5% N_2 -Ar plasma. Gaseous oxygen was injected through a septum into the carrier flow of the ETV to simulate the oxygen from the sample matrix, and the intensity at mass 32 was measured. The intensity at mass 32 appeared linearly proportional to the oxygen introduced ($r^2=0.997$). The sensitivity factor of oxygen in the 5% N_2 -Ar plasma is obtained from the slope of the curve to be 4 400 counts μmol^{-1} .

A linear instrument response to the sulfur concentration was substantiated by the correlation coefficient of 0.999 for calibration curves at both masses 32 and 34. Fig. 6 shows the signal profiles of a blank and a standard containing $0.5 \mu g g^{-1}$ of ^{32}S . The detection limits were 3.5 and $0.46 ng g^{-1}$ at masses 32 and 34, respectively, with a $20 \mu L$ sample volume. At the detection limits, the instrument responses were 6 300 and 860 counts at masses 32 and 34, respectively. If we accept that any signal of less than 6300 counts is not detected at mass 32, then the maximum amount of oxygen allowed in the sample without introducing a bias in a measurement is $1.4 \mu mol$.

The maximum amount of the sample matrix in the plasma without introducing a bias in the measurement can be estimated. Most samples are prepared with nitric acid for analysis by ICP-MS. Since nitrates readily decompose to metal oxides at temperatures above $300^\circ C$, oxides are the primary species after the pyrolysis step of the ETV. For a matrix element that forms a mono-oxide, the maximum concentration of the matrix element in the solution must be $<0.07 mol L^{-1}$. Thus for a sample of nickel alloy, for instance, the maximum concentration of the matrix is about 1% salt as a nitrate. This is a rather typical concentration for the matrix after samples are digested, suggesting that the ETV method for S may be adapted to most applications. In this work, sulfur in fossil fuels was determined by isotope dilution. Matrices of fossil fuels are not an oxygen source of concern since the digest of fossil fuels is essentially dilute nitric acid, which evaporates at the drying and pyrolysis steps.

Isotope dilution determination of S

Counting statistics is one factor that affects the precision of an isotope ratio measurement. It is an important limiting factor in the isotope ratio measurement with the ETV sampling system. The maximum number of counts that can be measured with the ETV sampling is limited by three factors. The first factor is the transient signal profile obtained with ETV, typically a skewed

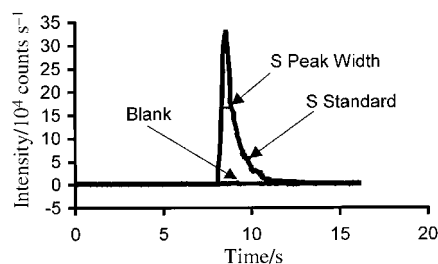


Fig. 6 Signal profiles of a blank and a $0.5 \mu g g^{-1}$ ^{32}S standard with a peak width of 0.7 s at half maximum.

Gaussian distribution with a full width at half maximum of about 1 s. This factor affords a finite number of counts with each firing. The second factor is the linear dynamic range of the detector that limits the peak intensity to about 10^6 counts s^{-1} . Lastly the duty cycle for measuring a specific isotope with a quadrupole ICP-MS is limited by the number of isotopes measured. Because a quadrupole mass spectrometer measures each isotope sequentially, the more isotopes that are measured, the less counts that are accumulated for each isotope. For this work, the sulfur peak width at half maximum, shown in Fig. 6, was about 0.7 s with the experimental instrument setting. Thus, the maximum number of counts that can be collected for a single isotope is about 7×10^5 counts assuming an upper limit of 10^6 counts s^{-1} for the linear dynamic range of the detector. For isotope ratio measurements, the maximum number of counts for each isotope is typically less than 4×10^5 since at least 2 isotopes are measured sequentially in the transient signal. For this maximum number of counts for each isotope of a ratio, the counting statistics precision can be no better than 0.22%; a significant background correction will further reduce the precision. Therefore, counting uncertainty is one of the major uncertainties for the ETV-based technique. A way to minimize this source of uncertainty is by averaging the isotope ratios of multiple firings of the ETV for the same sample, which was used for the IDMS measurement of S in this work.

The $^{32}\text{S}/^{34}\text{S}$ results for SRMs 2719 Petroleum Coke and 2724b Diesel Fuel are shown in the 3rd column of Table 2. Each ratio value in the column is an average of 6 replicate measurements. The 4th column lists the relative standard error (RSE, %) for the replicate measurements, which is the relative standard deviation of the 6 replicate measurements divided by square root of 6. The more precise TIMS values are also included in the 2nd column as a reference for each sample. The larger RSE of the unspiked samples (about 0.7%) relative to the spiked samples (about 0.3%) must be the result of poorer counting statistics at mass 34 than at 32, because the concentration of ^{32}S was prepared at about $0.3 \mu\text{g g}^{-1}$ for all samples.

The mass bias of the ICP-MS was corrected by measuring a solution of S having a $^{32}\text{S}/^{34}\text{S}$ ratio of 1.5764 determined by TIMS. As a result, the values of the sulfur isotope ratio by the two techniques can be compared. The $^{32}\text{S}/^{34}\text{S}$ values of the two techniques are in good agreement, indicated by the fact that the deviations of ETV values from those of TIMS are within the expanded RSE (95% confidence interval), which is calculated by multiplying the RSE by a coverage factor of 2.57. Again, the slightly larger deviation of about 0.7% observed for the unspiked SRM 2724b is attributable to the poorer counting statistics at mass 34 relative to that at mass 32.

In the determination of S in the fossil fuels, the single most significant source of uncertainty is the firing-to-firing variability of the ETV, which includes the counting uncertainty, signal profile distortion uncertainty and the background variability at the analyte masses. This uncertainty is reflected in the precision of the isotope ratio measurement. The average precision in terms of RSE for the $^{32}\text{S}/^{34}\text{S}$ ratio of the unspiked and spiked samples in Table 2 is 0.67% and 0.29%, respectively. Using $^{32}\text{S}/^{34}\text{S}$ ratio of 22.8 and 1.7 for the unspiked and the spiked samples, the RSE (1σ) of the determined concentration of S is estimated to be 0.32%. Table 3 lists the calculated

Table 2 Isotope ratio results for SRMs 2719 and 2724b

Sample ID	$^{32}\text{S}/^{34}\text{S}$ -TIMS	$^{32}\text{S}/^{34}\text{S}$ -ETV	RSE (%)	Deviation (%)
2719	22.71	22.67	0.78	-0.19
2719-spike1	2.165	2.169	0.29	0.18
2719-spike2	1.489	1.487	0.41	-0.15
2724b	22.71	22.88	0.55	0.73
2724b-spike1	1.181	1.180	0.33	-0.05
2724b-spike2	1.962	1.966	0.11	0.23

Table 3 S concentration in SRMs 2719 and 2724b ($\mu\text{g g}^{-1}$)

Sample ID	ETV	TIMS	Deviation (%)
2719-spike1	8904	8881	0.26
2719-spike2	8841	8843	-0.02
2724b-spike1	430.0	430.2	-0.05
2724b-spike2	431.2	430.1	0.25

S concentrations for the two methods. The S concentrations by the ETV method are within 0.3% of those by the TIMS method.

Conclusion

The background intensity at sulfur masses is greatly reduced by using ETV sample introduction for ICP-MS. However, the spectral background at mass 32 is still too high for the $^{32}\text{S}/^{34}\text{S}$ measurement to be successful. The use of a 5% N_2 -Ar plasma further reduces the background intensity at mass 32, making possible the accurate measurement of $^{32}\text{S}/^{34}\text{S}$. The results of sulfur in fossil fuels by the ETV technique are in good agreement with those by TIMS. The fundamental statistical limitations of the ETV method suggest that it will not be as precise as TIMS and therefore unlikely to supplant TIMS as a primary method for the element. Nevertheless, the ETV technique enjoys an advantage over TIMS in terms of higher analysis throughput and minimum sample preparation because a reduction of S^{6+} to S^{2-} is not needed for the ETV technique.²⁶

References

- Fed. Regist.*, 1999, **64**, 26004.
- D. P. Pope and C. T. Liu, in *Superalloys, Supercomposites and Superceramics*, ed. J. K. Tien and T. Caulfield, Academic Press, New York, 1989.
- K. Tsunoyama, in *Ultra High Purity Base Materials*, ed. K. Abiko, K. Hirokawa and S. Takaki, Japan Institute of Metals, 1995.
- J. R. Moody and M. S. Epstein, *Spectrochim. Acta, Part B*, 1991, **46**, 1571.
- W. R. Kelly, L. Chen, J. W. Gramlich and K. E. Hehn, *Analyst*, 1990, **115**, 1019.
- W. R. Kelly, P. J. Paulsen, K. E. Murphy, R. D. Vocke and L. Chen, *Anal. Chem.*, 1994, **66**, 2505.
- S. H. Tan and G. Horlick, *Appl. Spectrosc.*, 1986, **40**, 445.
- A. A. Menegário and M. F. Giné, *J. Anal. At. Spectrom.*, 1997, **12**, 671.
- A. A. Menegário, M. F. Giné and J. A. Bendassolli, *J. Anal. At. Spectrom.*, 1998, **13**, 1065.
- Technical Summary*, TSMS-12, Perkin-Elmer, 1991.
- J. Riondato, F. Vanhaecke, L. Moens and R. Dams, *J. Anal. At. Spectrom.*, 1997, **12**, 933.
- T. Prohaska, C. Latkoczy and G. Stingeder, *J. Anal. At. Spectrom.*, 1999, **14**, 1501.
- P. R. D. Mason, K. Kaspers and M. J. van Bergen, *J. Anal. At. Spectrom.*, 1999, **14**, 1067.
- D. C. Gregoire, *Prog. Anal. Spectrosc.*, 1989, **12**, 433.
- D. C. Gregoire and H. Naka, *J. Anal. At. Spectrom.*, 1995, **10**, 823.
- H. Naka and D. C. Gregoire, *J. Anal. At. Spectrom.*, 1996, **11**, 359.
- L. L. Yu, W. R. Kelly and J. D. Fassett, *J. Anal. At. Spectrom.*, in preparation.
- A. Montaser and H. Zhang, in *Inductively Coupled Plasma Mass Spectrometry*, ed. A. Montaser, Wiley-VCH, 1998.
- J. W. H. Lam and G. Horlick, *Spectrochim. Acta, Part B*, 1990, **45**, 1313.
- J. M. Craig and D. Beauchemin, *J. Anal. At. Spectrom.*, 1992, **7**, 937.
- S. R. Koirtyohann, J. S. Jones, C. P. Jester and D. A. Yates, *Spectrochim. Acta, Part B*, 1981, **36**, 49.
- D. J. Douglas and J. B. French, *J. Anal. At. Spectrom.*, 1988, **3**, 743.
- R. Campargue, *J. Chem. Phys.*, 1970, **52**, 1795.
- A. Kh. Gilmudinov, A. E. Staroverov, D. C. Gregoire, R. E. Sturgeon and C. L. Chakrabarti, *Spectrochim. Acta, Part B*, 1994, **49**, 1007.
- D. C. Gregoire, D. M. Goltz, M. M. Lamoureux and C. L. Chakrabarti, *J. Anal. At. Spectrom.*, 1994, **9**, 919.
- P. J. Paulsen and W. R. Kelly, *Anal. Chem.*, 1984, **56**, 708.